



Journal of Urban and Environmental
Engineering

E-ISSN: 1982-3932

celso@ct.ufpb.br

Universidade Federal da Paraíba
Brasil

Akhatova, A.; Kassymov, A.; Kazmaganbetova, M.; Rojas-Solórzano, L.
CFD SIMULATION OF THE DISPERSION OF EXHAUST GASES IN A TRAFFIC-
LOADED STREET OF ASTANA, KAZAKHSTAN
Journal of Urban and Environmental Engineering, vol. 9, núm. 2, 2015, pp. 158-167
Universidade Federal da Paraíba
Paraíba, Brasil

Available in: <http://www.redalyc.org/articulo.oa?id=283243518009>

- How to cite
- Complete issue
- More information about this article
- Journal's homepage in redalyc.org

redalyc.org

Scientific Information System

Network of Scientific Journals from Latin America, the Caribbean, Spain and Portugal

Non-profit academic project, developed under the open access initiative

CFD SIMULATION OF THE DISPERSION OF EXHAUST GASES IN A TRAFFIC-LOADED STREET OF ASTANA, KAZAKHSTAN

A. Akhatova*, A. Kassymov, M. Kazmagambetova and L. Rojas-Solórzano

Dept. of Mechanical Eng., School of Engineering, Nazarbayev University, Astana, 010000, Rep. of Kazakhstan

Received 23 August 2013; received in revised form 9 June 2015; accepted 31 October 2015

Abstract:

The aim of this paper is to consider one of the most traffic-loaded regions of Astana city (Kazakhstan) and to determine the concentration of carbon-monoxide (CO) in the air during the peak hours. CFD analysis based on the SolidWorks-EFD platform was used to simulate the dispersion of contaminants given the estimated emission rates and weather conditions at the crossroad of Bogenbay Batyr and Zhenis Avenues in Astana. Turbulence prediction was based on k- ϵ model with wall functions. The governing equations were discretized using the finite volume method and a 2nd order spatial scheme. The mesh verification was based on 1% convergence criterion for a 50% of mesh density increment; air pressure near the wall of a selected building was chosen as the parameter to control the convergence. Numerical results are presented for prevailing conditions during all 4 seasons of the year, demonstrating that the highest levels of CO are recorded in summer and reach the values up to 11.2 ppm which are still lower than the maximum level admitted for humans. Nevertheless, obtained results show that Astana is gradually becoming a city that is likely to reach the critical levels of pollutants in the nearest future if control measures are not taken with enough anticipation. As for a future work, it is proposed to perform in-situ validation of specific scenarios to check and support the results obtained with CFD and to develop then specific policies for tackling the problem before it becomes evident.

Keywords: CFD; Air pollution; Traffic Emissions; Street Canyon; SolidWorks

© 2015 Journal of Urban and Environmental Engineering (JUEE). All rights reserved.

NOMENCLATURE

C	Mass concentration	α	Thermal diffusivity
C_b	Mass concentration of the air	ϵ	Turbulent energy dissipation rate
CO	Carbon monoxide	f_μ	Turbulence damping factor
D	Molecular diffusive coefficient	g_i	Gravity vector
D^T	Turbulent diffusive coefficient	h	Height
I	Turbulent intensity	k	Specific turbulent energy
Le	Lewis number	μ	Dynamic viscosity
N_i	Number of cells in i direction	μ_t	Turbulent eddy viscosity
$N-E$	North-East	q	Diffusive heat flux
P	Pressure	ρ	Density
P_B	Turbulent generation due to buoyancy	τ	Shear stress
Pr	Prandtl Number	u_i	Velocity in i direction
$S-W$	South-West	δ_{ij}	Delta Kronecker
T	Temperature		

* Correspondence to: A. Akhatova. E-mail: aakhatova@nu.edu.kz

INTRODUCTION

Atmospheric air pollution in urban areas is one of the constantly discussed and monitored problems in the world in the last decades. With the growing need for heat and electricity and steadily rising number of vehicles, the young capital Astana is also becoming polluted with toxic gases. This implicates potential acute chronic health effects to the current 850,410 inhabitants of the city (Baik *et al.*, 2003; Darr & Vanka, 1991). The fact that city is under active construction at the moment makes it reasonable to study the dispersion of the toxic gases in the canyons of streets.

The results of such study will be useful for several reasons. Firstly, the general profile of toxic gas distribution will be generated for different meteorological conditions, which will allow to judge on the air quality in the city depending on the season of the year. This will contribute to the ecological study of the region. Secondly, the areas of high concentration of pollutants will be predicted (if there are any) in order to take measurements there and check if the concentration of exhaust gases is beyond the accepted norms. This information may also be considered by civil engineers which work on planning the city, particularly on the layout of buildings and roads. Finally, the results of this study may help engineers developing ventilation systems for neighboring buildings to optimize the location and design of HVAC inlets and outlets (Drivas and Shair, 1974).

The dispersion in built-up urban areas is classified as micro-scale dispersion, which refers to the dispersion processes less than 5 km in horizontal scale (Gousseau, 2011). The main difficulty in such studies is that the shape of the building affects the flow significantly. Complex geometries can produce intense turbulence, recirculation, reattachment, and dead zones. Therefore, it is very important to simplify the model moderately, by assuming the street canyon as an isolated unit and introducing plain, but realistic building geometries. Another simplification is that the study uses steady-state model of meteorological conditions, which relies on the average values of main parameters over the period of interest. In reality, the weather data is highly volatile, i.e. time-dependent. Finally, the lack of information on the traffic load in specified region becomes the major obstacle for the accurate prediction of the contaminant dispersion rates. Thus, the calculations were based on several observations and similar scenarios in other countries.

Wind flow and pollution dispersion in urban areas have been studied intensively in the last 20 years (Baik *et al.* 2012). With the recent extensive development of computer science, Computational Fluid Dynamics became an indispensable tool in such research (Baik *et*

al., 2012). It allows encompassing the larger scale models and with significantly reduced financial expenditures on research, as compared to the wind tunnel experimentation. Furthermore, a well-tuned CFD simulation will produce accurate results for every single point of the domain examined. However, the process of grid resolution and iterative convergence is time-consuming and the results are highly dependent on the accuracy of the input data.

There are many research works that simulated the dispersion in the street canyon on various software and applying different methodologies; they are discussed in more detail in the next section. In this study, Bogenbay Batyr and Zhenis streets' crossroad region was reproduced in CAD and then discretized using the finite volume method and a 2nd order upwind spatial scheme on the platform of DSS SolidWorks-EFD 2014, a powerful multifunctional CFD tool.

The wind flow trajectories and concentration of contaminant within the computational domain are studied for two seasons (summer and winter). The prevailing direction and magnitude of wind for each particular season are the main variable parameters. The street canyon is a crossroad, which is not a trivial case and represents a challenge to model. The results are used then in the diagnosis on the level of air pollution.

LITERATURE REVIEW

Extended research was conducted on the effects of urban landscape on the dissipation of atmospheric pollution since it became an evident issue in the last decades (Bitan, 1992). Vardoulakis *et al.* (2003), Johnson *et al.* (1973), Dabberdt *et al.* (1973), to mention a few authors, were among the first to describe the principles of distribution of polluting contaminants in city street canyons.

The breakthrough advances in computer technology in mid-1970s also led to the rapid development of research in the area. However, CFD modelling is not the only method in the field; for example, in some situations, full-scale field and wind tunnel experiments are valid tools to achieve indispensable information about the flow behavior. Many times a hybrid approach is the way to go, as for instance, in their recent work, the TRAPOS (acronym for Traffic Pollution in Streets) European research network did (Berkowicz, 2001). TRAPOS network of researchers combines continuous field contamination sampling, wind tunnel simulations and advanced mathematical (CFD) model calculations to attempt several common issues related to the urban areas. The network touches the thermal effects on flow stream and pollutant dispersion, the transformation of emitted contaminants, the turbulence due to the traffic

and the dependence of the flow on the geometry for a given location (Vardoulakis *et al.*, 2003).

The numerical approach work of several investigators (Vardoulakis *et al.*, 2013; DePaul and Sheih's, 1985; and Hoydysh and Dabbertdt, 1988) focuses on the research of transverse winds in street canyons, concluding that the concentrations of pollutants are higher on the leeward upwind side of the canyon. These works show that the windward concentration is usually about 2 times lower than the leeward one. Authors then proceed to assess the cases with the direction of wind parallel to the street, claiming that in such conditions the highest contaminant concentrations are achieved (Vardoulakis *et al.*, 2002). Finally, previous works refer to several studies (Qin and Kot, 1993; Vignati *et al.*, 1996; Jones *et al.*, 2000; and DePaul and Sheih, 1986) stating that low wind conditions precipitate the accumulation of pollutants.

MODEL SET-UP

Physical Model

There are several unique combinations to set up the dynamics of external flows in CFD models. SOLIDWORKS Flow Simulation tool requires several governing equations and parameters to be specified, which, in this study, are the Reynolds-Averaged Navier-Stokes (RANS) equations, ideal gas, mass, energy and conservation of species equations, and the added closure 2-equation enhanced k- ϵ turbulence model. The latter is a combination of classical k- ϵ model and Launder-Spalding wall function approach (SolidWorks Flow Simulation Technical Paper, 2013).

An idealized model with two intersecting dense traffic street canyons at 1:1 scale was built in SolidWorks CAD program (Fig. 1). Buildings present in this model are similar in shape and size to their real analogs and are positioned accordingly using satellite images of the area. The ground plate is added only for visualization purpose and is not added to the computational domain.

Computational Domain

The computational domain for this study is shown in Fig. 2. It has a shape of rectangular prism with the dimensions of 800×800×210m. The boundary planes of computational domain and its coordinate system are adjusted in accordance with the wind direction entering the region, so that Z-direction always coincides with the wind direction. The height of the computational domain was taken in accordance with the conventions established by previous CFD analyses, by which it

should not be less than five times the maximum height of the buildings (Kim, 2013).

The domain is surrounded by boundaries at atmospheric pressure except the entrance, where a developed turbulent flow profile is prescribed with the prevailing wind direction (Gromke and Ruck, n.d.). In accordance with estimated average seasonal wind directions, flow enters the domain at the left side in summer and at the right side in other seasons as it is shown in Fig. 2. Trees and other small obstacles were neglected due to their sparse distribution and small length scale in comparison with the buildings.

The inflow and outflow boundaries are 110 meters away from the upwind and downwind buildings respectively, to guarantee enough space for the flow to adjust to the constant pressure and fully

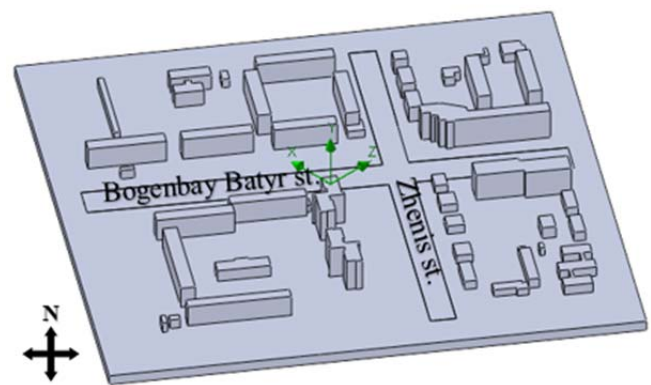


Fig. 1 Physical model.

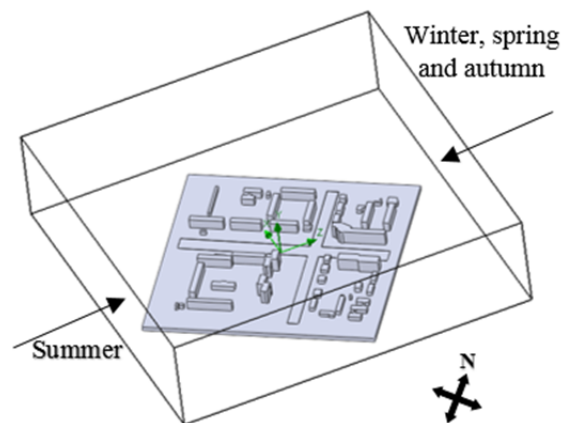


Fig. 2 Computational domain.

developed condition at outflow boundaries. Also, the streets having the dimensions of 400×25m and 400×32m (Zhenis and Bogenbay Batyr, respectively) are indicated in the model. The line sources at the surface level were added along them to account for tracer gas emissions.

Pollutant Mass Flow

The decision to study the dispersion of carbon monoxide (CO) is based on the highest level of toxicity

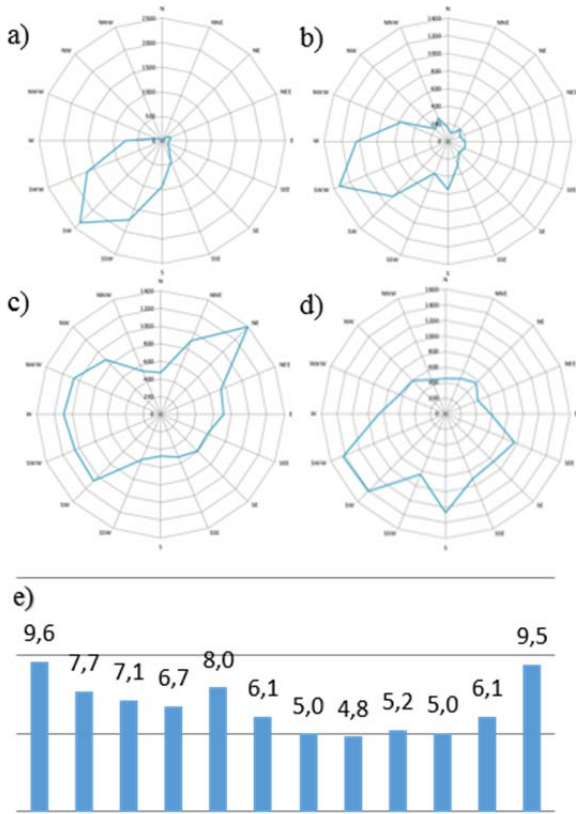


Fig. 3 Wind potential in Astana: wind roses for (a) winter, (b) spring, (c) summer, (d) autumn; (e) wind speed by months (January-December).

of the gas among other components of automobile exhaust. The following data on its properties was found in order to calculate the gas mass flow rate for the tracer study: molar mass = 28.011 g/mol (Engineering Toolbox, 2014), diffusion coefficient of CO in air = $0.202 \times 10^{-4} \text{ m}^2/\text{s}$ at 300K and 1 atm (Dean, 1999). The total mass flow rate was then calculated using the estimated average number of vehicles in the area, average traffic speed in Astana in mornings and evenings and average car emissions per unit distance information (US EPA, 2008).

The information on the wind speed and direction in Astana was found in the wind potential database from UNDP/GEF wind energy project's archive (KEA, 2007). Based on that the wind roses were built (**Fig. 3**).

Mathematical Model

The mathematical model is based on the set of governing equations and respective boundary conditions. The main premises are: steady state, Newtonian fluid, incompressible and turbulent flow. Therefore, the following Favré-averaged governing equations and boundary conditions were prescribed: (a) mass conservation; (b) Navier-Stokes (momentum) equations; (c) energy conservation; (d) constitutive relations between p , T and H ; (e) species conservation;

and (f) k - ϵ turbulence model with wall functions. These equations are shown as follows:

$$\frac{\partial \rho}{\partial t} + \frac{\partial}{\partial x_i}(\rho u_i) = 0 \quad (1)$$

$$\frac{\partial \rho u_i}{\partial t} + \frac{\partial}{\partial x_j}(\rho u_i u_j) = -\frac{\partial p}{\partial x_i} + \frac{\partial}{\partial x_j}(\tau_{ij} + \tau_{ij}^R); i = 1, 2, 3 \quad (2)$$

with:

$$\tau_{ij} = \mu \left(\frac{\partial u_i}{\partial x_j} + \frac{\partial u_j}{\partial x_i} - \frac{2}{3} \delta_{ij} \frac{\partial u_k}{\partial x_k} \right) \quad (3)$$

(Newtonian fluid to turn the momentum equations into Navier-Stokes equations).

$$\tau_{ij}^R = \mu_t \left(\frac{\partial u_i}{\partial x_j} + \frac{\partial u_j}{\partial x_i} - \frac{2}{3} \delta_{ij} \frac{\partial u_k}{\partial x_k} \right) - \frac{2}{3} \rho k \delta_{ij} \quad (4)$$

(Boussinesq's assumption for the Reynolds-stress).

where, δ_{ij} is the Kronecker delta function, μ is the dynamic viscosity, μ_t is the turbulent eddy viscosity and k is the specific turbulent kinetic energy.

The energy transport equation for the fluid in terms of enthalpy:

$$\frac{\partial \rho H}{\partial t} + \frac{\partial \rho u_i H}{\partial x_i} = \frac{\partial}{\partial x_i} \left(u_j (\tau_{ij} + \tau_{ij}^R) + q_i \right) + \frac{\partial p}{\partial t} - \tau_{ij}^R \frac{\partial u_i}{\partial x_j} + \rho \epsilon + S_i u_i + Q_H \quad H = h + \frac{u^2}{2} \quad (5)$$

For the air flow, the Ideal Gas state equation is prescribed to compute its density as a function of pressure and temperature:

$$\rho = \frac{p}{R_{air} T} \quad \text{with} \quad R_{air} = \frac{R_{universal}}{Air_Molecular_Mass} \quad (6)$$

The species transport equation on background fluid (in this paper, contaminants on background air):

$$\frac{\partial \rho C}{\partial t} + \frac{\partial \rho u_i C}{\partial x_i} = \frac{\partial}{\partial x_i} \left((D + D^T) \frac{\partial C}{\partial x_i} \right) \quad (7)$$

with:

$$D^T = \frac{\mu_t}{\sigma} \quad (8)$$

$$C + C_b = 1 \quad (9)$$

where C is the mass concentration of the species (contaminant) diffusing in the background fluid (air), C_b is the mass concentration of air, D , D^T are the molecular and turbulent diffusive coefficients, respectively, of the

species on the background fluid. Also, u is the time-averaged fluid velocity, ρ is the fluid density, p is the time-averaged fluid pressure, h is the enthalpy, τ_{ij} is the viscous stress tensor or the Reynolds stress tensor when accompanied by superscript "R", q_i is the diffusive heat flux.

The additional k - ε transport equations for the specific turbulent kinetic energy and dissipation, respectively:

$$\frac{\partial \rho k}{\partial t} + \frac{\partial}{\partial x_i} (\rho u_i k) = \frac{\partial}{\partial x_i} \left(\left(\mu + \frac{\mu_t}{\sigma_k} \right) \frac{\partial k}{\partial x_i} \right) \quad (10)$$

$$\frac{\partial \rho \varepsilon}{\partial t} + \frac{\partial}{\partial x_i} (\rho u_i \varepsilon) = \frac{\partial}{\partial x_i} \left(\left(\mu + \frac{\mu_t}{\sigma_\varepsilon} \right) \frac{\partial \varepsilon}{\partial x_i} \right) \quad (11)$$

where, the source terms are defined as:

$$S_k = \tau_{ij}^R \frac{\partial u_i}{\partial x_j} - \rho \varepsilon + \mu_t P_B \quad (12)$$

$$S_\varepsilon = C_{\varepsilon 1} \frac{\varepsilon}{k} \left(f_1 \tau_{ij}^R \frac{\partial u_i}{\partial x_j} + \mu_t C_B P_B \right) - C_{\varepsilon 2} f_2 \frac{\rho \varepsilon^2}{k} \quad (13)$$

where, P_B represents the turbulence generation due to buoyancy forces and is given by:

$$P_B = -\frac{g_i}{\sigma_B} \frac{1}{\rho} \frac{\partial \rho}{\partial x_i} \quad (14)$$

with $g_i = (g_x, g_y, g_z)$ the gravity vector, the constant $\sigma_B=0.9$ and constant $C_B = 1$ when $P_B > 0$, and 0 otherwise. Whereas:

$$f_1 = 1 + \left(\frac{0.05}{f_\mu} \right)^3 \quad \text{and} \quad f_2 = 1 - \exp(-R_t^2) \quad (15)$$

The constants C_μ , $C_{\varepsilon 1}$, $C_{\varepsilon 2}$, σ_k , σ_ε are obtained from typical fitting experiments as:

$$C_\mu=0.09, C_{\varepsilon 1}=1.44, C_{\varepsilon 2}=1.92, \sigma_k=1, \sigma_\varepsilon=1.3 \quad (16)$$

For Lewis number ($Le = \alpha/D$), $Le=1$, the diffusive heat flux is defined as:

$$q_i = \left(\frac{\mu}{Pr} + \frac{\mu_t}{\sigma_\varepsilon} \right) \frac{\partial h}{\partial x_i} \quad (17)$$

with the constant $\sigma_\varepsilon = 0.9$, Pr is the Prandtl number, α is the thermal diffusivity and D is the mass diffusivity. And the relation between k , ε and μ_t is given by:

$$\mu_t = f_\mu \frac{C_\mu \rho k^2}{\varepsilon} \quad (18)$$

and f_μ is a turbulence damping factor to consider the laminar-turbulent transition as a function of distance from the wall, defined by the expression:

$$f_\mu = \left[1 - \exp(-0.025 R_y) \right]^2 \cdot \left(1 + \frac{20.5}{R_y} \right) \quad (21)$$

where:

$$R_r = \frac{\rho k^2}{\mu \varepsilon} \quad \text{and} \quad R_y = \frac{\rho \sqrt{k} y}{\mu} \quad (19)$$

and y is the distance from the wall.

Boundary Conditions

According to the wind rose the direction of prevailing winds changes twice per year: S-W winds dominate during summer period, while for the rest of the year averaged winds blow in opposite direction. Therefore, a "free flow (wind) speed U " is set as inlet velocity boundary condition; the wind profile takes the shape shown in **Fig. 4** with the profile equation given by:

$$V_y = V_h \left(\frac{y}{h} \right)^n \quad (20)$$

where V_h is the velocity at the height h and n is 0.25 for all cases (RLS Energy, 2014).

Table 1 shows the average velocities at the height of 50 meters, directions of the prevailing wind, and average temperatures for four seasons. The surfaces of the buildings are adiabatic, smooth and set to no-slip

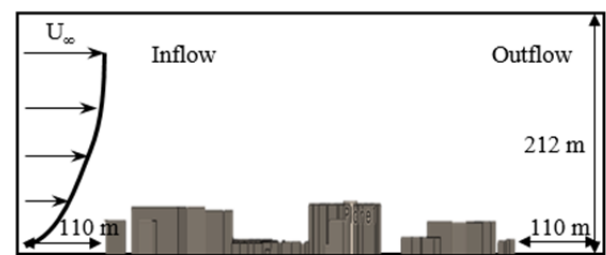


Fig. 4 Wind profile boundary condition.

Table 1. Average meteorological data for 4 seasons in the city of Astana (Weather Spark, 2014)

Seasons	Winter	Spring	Summer	Fall
Average Velocity (h = 50m, m/s)	8.93	7.27	5.3	5.43
Direction of the wind	S-W	S-W	N-E	S-W
Average Temperature (K)	256.2	277.2	293.2	278.2

condition. The boundary conditions on the example of summer are schematically indicated in **Fig. 5**.

The outlet flow is stable both thermally and hydrodynamically, and the velocity profile is developed:

$$\frac{d\bar{v}}{d\bar{n}} = 0 \quad (21)$$

Other boundary conditions are given as follows: (a) gas emissions are set to 0 at domain inlet, and there are no emissions (species) flux through the walls of buildings; (b) the concentration of emissions is set to 1 at the street surfaces to simulate car exhausts.

Turbulence parameters are defined in terms of turbulence intensity I and the length scale of largest expected eddies. These values are set by default as 0.1% and 0.4191m.

Discretization of Governing Equations

The discretization of governing equations is based on the finite volume (FV) method applied locally at solid/fluid interfaces and in the regions where high gradients are expected. The FV method grants the conservative discretization of the governing equations, with spatial derivatives (fluxes) approximated with second-order upwind on the implicitly treated modified Leonard's QUICK (Quadratic Upstream Interpolation of Convective Kinematics) (Roache, 1998) and a Total Variation Diminishing (TVD) method (Hirsch, 1988).

An operator-splitting technique (Glowinski and Le Tallec, 1989; Marchuk, 1982; and Samarskii, 1989), which follows SIMPLE algorithm described by Patankar (1980), is applied to efficiently resolve the problem of pressure-velocity decoupling.

The resulting linearized algebraic system of equations is then solved iteratively on the LU-factorization preconditioned matrix using the generalized conjugate gradient method (Saad, 1996). The stop criterion of the solver is achieved when the difference in average pressure values at selected wall in two consecutive iterations becomes less than 0.01%.

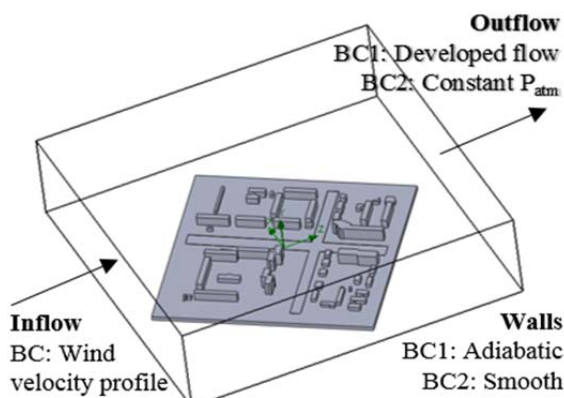


Fig. 5 Computational domain with boundary conditions shown.

Mesh Sensitivity Analysis

The computational mesh was optimized by the refinement of cells in high-gradient flow regions and merging the cells in low-gradient flow regions. This results in better accuracy of the results. 4 levels of mesh refinement were considered: coarse mesh containing 20 778 cells, two medium meshes with 29 447 and 45 174 cells, and the finest mesh with 68 334 cells in it (**Fig. 6**).

Four meshes shown in **Fig. 6** above were used for the Mesh Sensitivity Analysis (MSA). Convergence control is based on the averaged value of maximum static pressure on leeward surfaces of buildings. The mesh independence criterion is specified such that the analysis stops when a 50% refinement of the mesh leads to 0.01% or smaller difference in pressure.

After the simulation with the fourth mesh it was found that the difference in pressure in two last runs was within 0.01%. For the sake of accuracy the finest mesh was selected for the remaining numerical tests. The table below shows the summary of the data obtained on four meshes containing the information about the number of elements and differences in main parameter values in consecutive mesh verification steps.

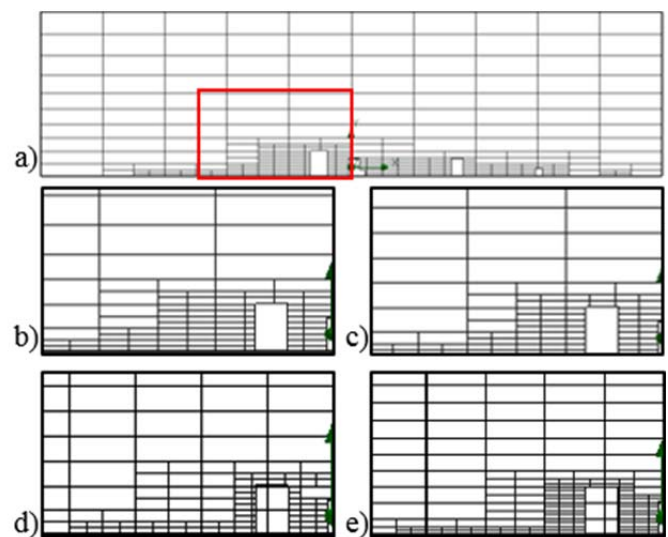


Fig. 6 Meshes used for MSA: (a) coarse mesh (cut plot along windward face), (b) Mesh 1 zoomed, (c) Mesh 2 zoomed, (d) Mesh 3 zoomed, (e) Mesh 4 zoomed.

Table 2. Summary of Mesh Sensitivity Analysis

	Total number of cells	Analysis duration (s)	Pressure (Pa)	Delta (%)
Mesh 1	20 778	251	101 392	
Mesh 2	29 477	294	101 409	0.0168
Mesh 3	45 174	366	101 377	0.0315
Mesh 4	68 334	340	101 371	0.0059

Model Validation

The main challenge to the CFD pollution model based on the turbulent dispersion of species in street canyons is associated with the typical obstacle-based geometry, in which the detachment and reattachment of boundary layer occurs, thus generating complex flow streamline patterns. The lid-backward-facing step is recognized by many authors as the standard test to validate the turbulence models for these applications (i.e., Sahm *et al.*, 2002; Vardoulakis *et al.*, 2003; Chu *et al.*, 2005). Additionally, it was demonstrated that k- ϵ turbulence model is usually the choice (e.g. Ketzal *et al.*, 2002) due to the convenient compromise between its computational economy, robustness and accuracy.

In this investigation, proposed CFD model, based on the enhanced k- ϵ turbulence closure, was previously validated on lid-driven 2D recirculating flows (Michelsen *et al.*, 1986) in closed 2D triangular and trapezoidal cavities with one or two moving lids (Darr *et al.*, 1991), demonstrating accurate predictions of the fundamental flow features (SolidWorks Flow Simulation Technical Paper, 2013).

Computational Equipment

The simulations were performed on a computer with following parameters: CPU: Intel Core i5-3210M @2.50GHz; RAM: 4.00 GB; HDD: 750 GB @ 5400 rpm.

It is important to mention several factors that led to additional improvement of computational performance: relatively small size of the area of interest, several simplifications applied to the model geometry and properties and the fact that the model consists of one part only. As a result, good performance was achieved, and that allowed using the fine mesh to obtain the most accurate results with reasonable time and memory expenditures: in average it took about 6 minutes to reach the convergence of parameters.

RESULTS

The wind streamlines for four seasons are shown in **Fig. 7** below. It supports initial expectations about the presence of vortices and recirculations and overall reduction in the wind velocity due to buildings. Since the height at which streamlines enter the computational domain equal 1.5 m, it can be concluded that although the flow bypasses high buildings laterally it, at the same time, possesses enough kinetic energy to cross lower ones without circumventing them. Finally, it is clearly seen that in each case there is a massive air flow along Bogenbay Batyr avenue canyon, which follows the prevailing direction of wind quite well.

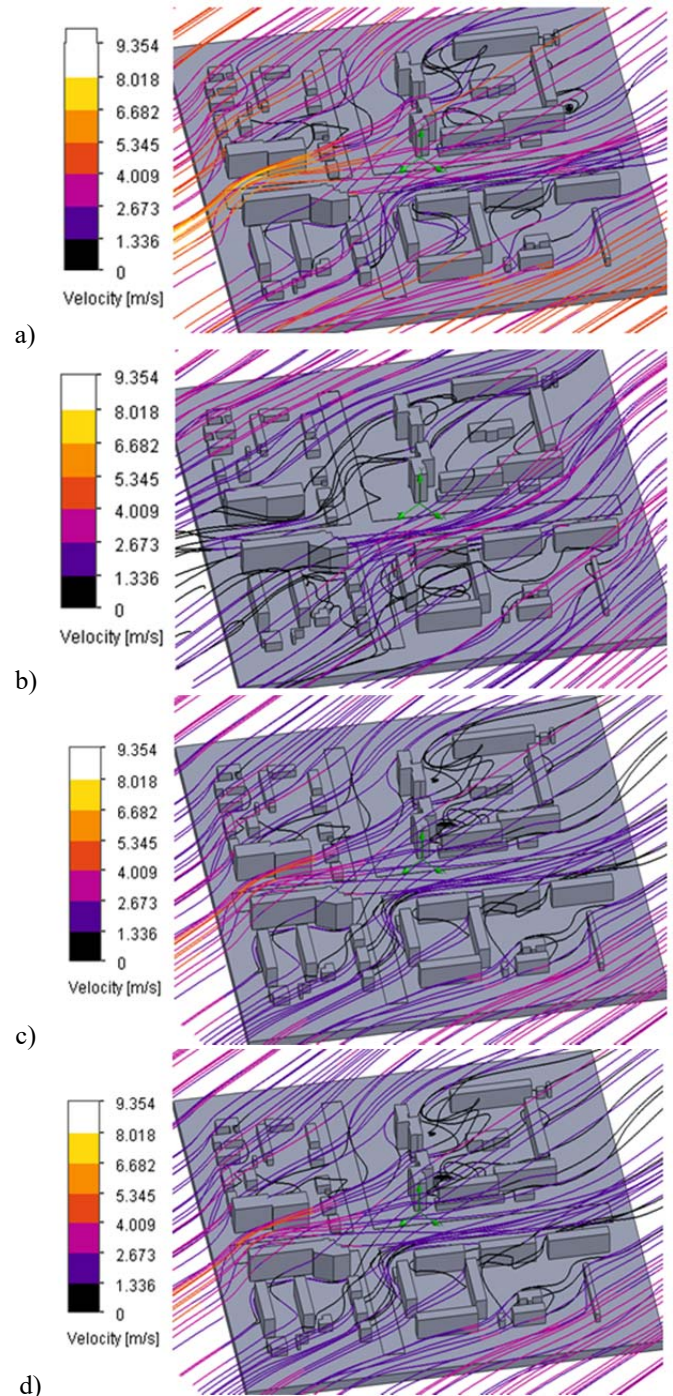


Fig. 7 Flow streamlines for different seasons: (a) Winter, (b) Spring, (c) Summer, (d) Autumn.

The carbon monoxide mass concentration of 3 ppm (parts per million), was chosen as a basis to compare four cases. **Figure 8** displays pollutant concentration isosurfaces corresponding to this concentration. In four scenarios the order of maximum mass fraction of the dispersed gas mixture is 10^{-6} , only differing by a small amount. **Figure 9** illustrates the concentration contour cut plots at 1.5 m above the ground level.

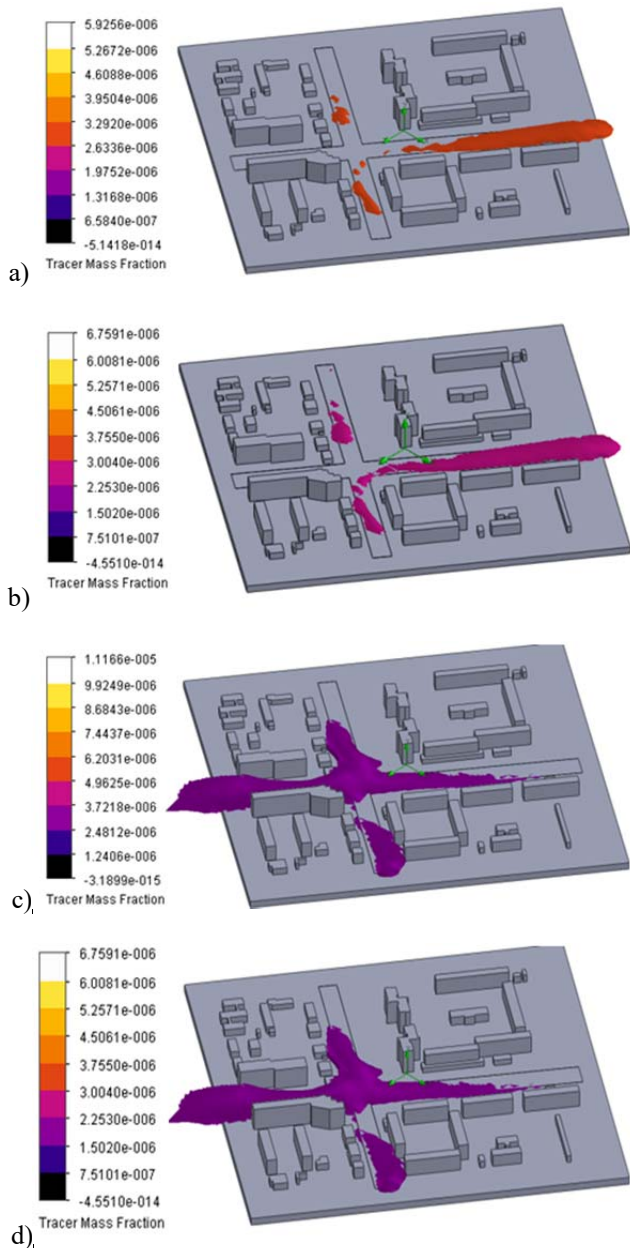


Fig. 8 Isosurfaces of CO mass fraction in different seasons: (a) Winter, (b) Spring, (c) Summer, (d) Autumn.

The results of the study show that the maximum concentration of carbon monoxide, observed in the domain under given conditions, is not hazardous for citizens' health, unless they are very close to the contaminant source for a long time. According to US Federal Highway Administration, the maximum allowed impact of the gas is achieved during the exposure at 35 ppm for 1 hour or 9 ppm for 8 hours (US Department of Transportation, 2011). Since the concentration of CO in the pedestrian areas in this study varies from 3.0 to 11.2 ppm, the probability of getting poisoned by the gas in the street is quite low. It is not hazardous for common people in transit, but could have negative effects on local residents or officers on duty.

There are several other points which can be mentioned based on obtained data. Firstly, because the buildings are quite distant from the road and are not too high, there are no

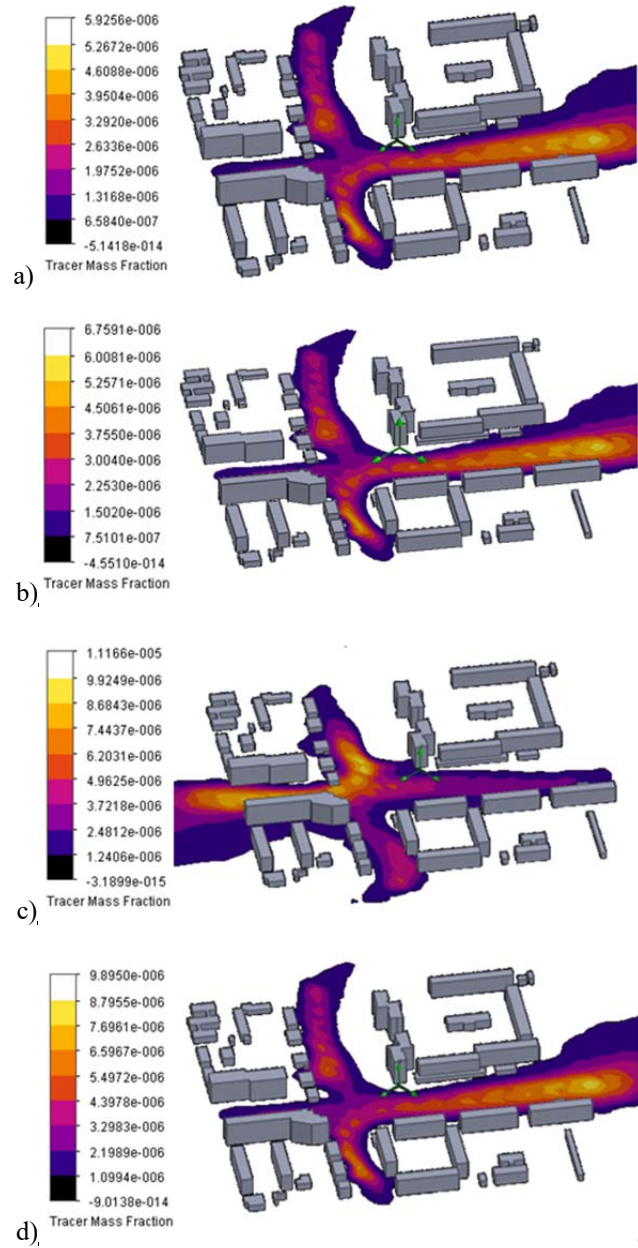


Fig. 9 Contour cut plots of pollutant dispersion: (a) Winter, (b) Spring, (c) Summer, (d) Autumn.

“contaminant stuck” regions, which are usually formed at the wakes of buildings.

Also, the buildings located in the south-western side of the domain are more subjected to emissions. It can be mentioned that the concentration of CO is higher in the leeward regions, which corresponds to earlier studies. Taking into account that NE winds prevail in Astana most of the year, this observation describes the phenomena, mentioned above.

The study supports the prediction about the types of the terrain with highest rates of contamination as well. In accordance with it, concentration of gases is significantly higher along the street canyons than in residential areas. This implies that mostly drivers, passengers, and pedestrians are affected by CO, rather than inhabitants of the apartments nearby.

Finally, it can be mentioned that the highest and lowest rates of contamination relate to summer and winter periods

respectively. The reason for such difference is the speed of wind, which is the highest in winter and the lowest in summer, as it was shown before. The effect of temperature and, thus, the density of gases on buoyancy should be considered as well. The difference in results for autumn and spring periods is very small because of the similar temperatures and wind directions and speeds.

CONCLUSIONS AND REMARKS

The study uses CFD approach to evaluate the dispersion of pollutants from automobile exhausts in the chosen area in the city of Astana and negative effects it may cause on local residents' health. According to obtained results the current level of pollution does not exceed the levels of 3.0 to 11.2 ppm, depending on the season, and thus the critical level is not normally achieved. The data obtained also supports several studies on pollution dispersion patterns in different terrains and at different ambient conditions.

In order to obtain more realistic results it is recommended to conduct a further, more thorough study implementing a larger, more sophisticated model of the city and take into account the contamination coming from the thermal plant, the number of complaints on operation of which rises year-by-year. The effects of several poisonous gases may be covered by the study to significantly improve its efficiency. Other turbulence intensity models may be tested to optimize and improve the method. Finally, the proper in-situ research is recommended to assess the accuracy of the approach and to prove its viability and further potential to local authorities.

Acknowledgment The authors would like to thank Professor Andrey Alyamovsky, from DSS Solidworks Russia, for kindly providing the materials, and supporting with hands-on guidance. Also many thanks to the students of Professor L.R.Rojas-Solorzano for providing with necessary data.

REFERENCES

- Baik, J., Kim, J.K., and Fernando, H.J. (2003). A CFD Model for Simulating Urban Flow and Dispersion. *Amer. Meteor. Soc.*, **42**(11), 1636-1648.
- Berkowicz, R. (2001) *The European Research Network TRAPOS - Results and Achievements*. DCE - Danish Centre For Environment And Energy. Resource document. <http://www2.dmu.dk>. Accessed 15 April 2014.
- Bitan, A. (1992) The High Climatic Quality City of The Future. *Atmos. Environ.*, **26**(3), 313-329.
- Brunekeerf, B. and Holgate, S.T. (2002) *The Lancet*, **360**, 1233 – 1242
- Carlson, D.J. and Hoglund, R.F. (1964) Particle Drag and Heat Transfer in Rocket Nozzles. *AIAA Journal*, **2**(11), 1980-1984.
- Chu, A.K.M., Kwok, R.C.W. and Yu, K.N. (2005) Study of Pollution Dispersion in Urban Areas Using Computational Fluid Dynamics (CFD) and Geographic Information System (GIS) *Environm. Model. Soft.*, **20**(2), 273-277.
- Dabberdt, L. and Johnson, D. (1973) Validation and applications of an urban diffusion model for vehicular pollutants. *Atmos. Environ.*, **7**(6), 603-618.
- Darr, J.H. and Vanka, S.P. (1991) Separated Flow in a Driven Trapezoidal Cavity. *Phys. Fluids: A Fluid Dyn.*, **3**(3), 385-392.
- Dassault Systems (2013) *Technical Reference: Solid Works Flow Simulation 2013*.
- Dean, J. (1999) *Lange's Handbook of Chemistry*. 15th ed. New York: McGraw-Hill.
- Department of Statistics of Astana. 2014. *About demographic situation in Astana*. Resource Document. <http://www.astana.stat.kz>. Accessed 29 January 2015.
- DePaul, F.T., Sheih, C.M. (1985) A tracer study of dispersion in an urban street canyon. *Atmos. Environ.*, **19**(4), 555-559.
- Drivas, P.J. and Shair F.H. (1974) A tracer study of pollutant transport and dispersion in the Los Angeles area. *Atmos. Environ.*, **8**(11), 1155-1163.
- Glowinski, R. and Le Tallec, P. (1989) Augmented Lagrangian Methods and Operator-Splitting Methods in Nonlinear Mechanics. *Studies in Applied and Numerical Mathematics*. doi: 10.1137/1.9781611970838.
- Gousseau, P., Blocken, B., Stathopoulos, T., van Heijst, G.J.F. (2011) CFD simulation of near-field pollutant dispersion on a high resolution grid: a case study by LES and RANS for a building group in downtown Montreal. *Atmos. Environ.*, **45**, 428-438.
- Gromke, C. and Ruck, B. (n.d.) *Flow and Dispersion Phenomena in Urban Street Canyons in the Presence of Trees*. Resource document. Institute for Hydromechanics: Karlsruhe Institute of Technology. <http://www.ifh.uni-karlsruhe.de>. Accessed 19 April 2014.
- Henderson, C.B. (1976) Drag Coefficients of Spheres in Continuum and Rarefied Flows. *AIAA Journal*, **14**(6), 707-708.
- Hirsch, C. (1988) *Numerical Computation of Internal and External Flows*. Chichester: John Wiley and Sons.
- Hoydysh, W.G., Dabberdt, W.F. (1988) Kinematics and dispersion characteristics of flows in asymmetric street canyons. *Atmos. Environ.*, **22**, 2677-2689.
- Johnson, W.B., Ludwig, F.L., Dabberdt, W.F., Allen R.J. (1973) An urban diffusion simulation model for carbon monoxide. *J. Air Poll. Control Assoc.*, **23**, 490-498.
- Jones, S.G., Fisher, B.E.A., Gonzalez-Flesca, N., Sokhi, R. (2000) The use of measurement programmes and models to assess concentrations next to major roads in urban areas. *Environ. Monit. Assess.*, **64**, 531-547.
- KEA (Kazakhstan Electricity Association) (2007) Committee of Renewable Resources. Resource Document. <http://www.windenergy.kz>. Accessed 10 April 2014.
- Ketzel, M., Berkowicz, R., Müller, W., Lohmeyer A. (2002) Dependence of street canyon concentrations on above roof wind speed – Implications for numerical modelling. *Int. J. Environ. Poll.*, **17**, 356-366.
- Kim, D. (2013) The Application of CFD to Building and Design: A Combined Approach of an Immersive Case Study and Wind Tunnel Testing. *Ph.D. Dissertation*. Resource Document. Virginia Polytechnic Institute and State University. <http://vtechworks.lib.vt.edu>. Accessed 12 April 2014.
- Marchuk, G.I. (1982) *Methods of Numerical Mathematics*. Berlin: Springer-Verlag.
- Michelsen, J.A. (1986) Modeling of Laminar Incompressible Rotating Fluid Flow. *AFM note*, **86**(5), 534-541.
- Patankar, S.V. (1980) *Numerical Heat Transfer and Fluid Flow*. Washington, D.C: Hemisphere.
- Qin, Y. and Kot, S.C. (1993) Dispersion of vehicular emission in street canyons, Guangzhou City, South China (P.R.C.) *Atmos. Environ.*, **27b**, 283-291.
- RLS Energy (2014) *Wind speed data. Adjusting wind speed*. Resource Document. <http://rlsenergy.com>. Accessed 13 April 2014.
- Roache, P.J. (1998) *Technical Reference of Computational Fluid Dynamics*. Albuquerque, New Mexico: Hermosa Publishers.
- Saad, Y. (1996) *Iterative methods for sparse linear systems*. Boston: PWS Publishing Company.
- Sahm, P., Louka, P., Ketzel, M., Guilloteau, E. and Sini, J.-F. (2002)

- Intercomparison of Numerical Urban Dispersion Models – Part I: Street Canyon And Single Building Configurations. *Water, Air Soil Poll.*, **2**(5-6), 587-601.
- Samarskii, A.A. (1989) *Theory of difference schemes*. Moscow: Nauka (in Russian).
- The Engineering Toolbox (2014) *Gases–Densities*. Resource Document. <http://www.engineeringtoolbox.com> Accessed 10 April 2014.
- United States Environmental Protection Agency (US EPA) (2008) Average Annual Emissions and Fuel Consumption for Gasoline-Fueled Passenger Cars and Light Trucks. Resource document. <http://www.epa.gov>. Accessed 19 April 2014.
- US Department of Transportation. (2011) Federal Highway Administration (FHWA) Carbon Monoxide (CO) Categorical Hot-Spot Finding. Resource document. <http://www.fhwa.dot.gov/>. Accessed 29 May 2014.
- Vardoulakis, S., Fisher, B., Pericleous, K. and Gonzalez-Flesca, N. (2002) Modelling air quality in street canyons: a review. *Atmos. Environ.*, **37**(2), p.155-182, 2004.
- Vignati, E., Berkowicz, R., Hertel O. (1996) Comparison of air quality in streets of Copenhagen and Milan, in view of the climatological conditions. *The Sci. Total Environ.*, **189/190**, 467-473.
- Weather Spark. (2014) *Average Weather For Astana, Kazakhstan*. Resource document. <http://weatherspark.com>. Accessed 18 April 2014.
- WebQC (2014) *Molar Mass, Molecular Weight, Elemental Composition Calculator*. Resource document. WebQC online portal. <http://www.webqc.org/> Accessed 15 April 2014.